International Journal of Applied Engineering Research ISSN 0973-4562 Volume 10, Number 23 (2015) pp 43649-43654

Study of Tensile and Corrosion Behaviour from the Microstructure of AZ91D Magnesium Alloy

R. Jayaraman

V. M. K. V. Engineering College, Salem, Tamilnadu, India

Dr. T. Balusamy

Government College of Engineering, Salem, Tamilnadu, India.

Dr. S. Ravi

Annamalai University, Chidambaram, Tamil Nadu, India

Abstract
This paper evaluates the micro-hardness and corrosion behavior of friction stir processed AZ91D magnesium alloy in the process of effecting fine grained structure. The yield strength, ultimate tensile strength, percentage of elongation of the base mental being cast along AZ91D of 12 mm thickness are analyzed the through tensile behavior and micro hardness properties and are studied and compared with the processed material of the same alloy composition. Scanning electron microscope was employed to analyze the microstructure of the studied alloys. The study further contrasts the tensile properties and micro hardness properties at the cross section of the base metal and the processed fine gained materials. The micro structural analysis is carried using optical metallographic and scanning electron microscope and the fine grained friction stir processed AZ91D magnesium alloy is further processed for equal channel angular pressing. The angular pressing method is exclusively used to carry out study of the corrosion behavior of material.

Keywords: Corrosion, Tensile behaviour, magnesium alloy, microstructure, friction, stir processing.

1. Introduction
Magnesium and its alloys have been widely used due to their excellent mechanical properties, actability and machin-ability. In earlier research, many paper [1-3] focused on the corrosion behavior of magnesium alloys as a result of their bad corrosion resistance which has restricted their application. Additionally, the relatively lower tensile strength of magnesium alloy is another important factor which limits their performances load-carrying members. Magnesium alloys are regarded as the green structural metallic materials for the 21st century, and have great potential in industrial applications, especially in aviation and transportation fields. However, their applications are still limited due to several undesirable properties, such as relative low strength, ductility and poor corrosion resistance. Since grain refinement is proved to be favorable to improving both mechanical properties and corrosion resistance of Mg alloys, significant efforts have been devoted to developing wrought Mg alloys with ultra-fine grains [4-5]. Herein, a new conceptual metal forming process-Equal-Channel Angular Pressing (ECAP) deserves attention as one of the most attractive grain-refining methods [6, 7]. The process has been widely investigated in the last decades for the efficient production of bulk ultrafine grained (UFG) materials via severe plastic deformation. Plenty of ECAP processed (ECAPed) metallic structural materials (e. g. Mg, Al, Fe, etc.) obtain exceptional mechanical or/and physical advantages [6-8], even enhanced corrosion resistance [9-11]. AZ91D Mg alloy with nominal composition Mg-9 wt% Al-1 wt% Zn is one of the most popular of cast Mg alloys.
The typical microstructure of cast AZ91D alloy consists of matrix a-Mg solid solution with segregated b-phase ($Mg_{17}Al_{12}$) along grain boundaries. The ECAP application in AZ91 alloy to improve mechanical properties has been reported in some researches [12]. The tensile yield strength was improved from 167 to 417 MPa of AZ91 alloy, thus the benefit of ECAP to enhance the mechanical property of AZ91 alloy was marked. In contrast, only limited attention was focused on the corrosion behavior of the ECAPed Mg alloys.
As well known, compared to other conventional metallic structural materials, Mg alloys have poor corrosion resistance in many environments, especially in Cl_-containing solutions. Although adding aluminium to Mg matrix will be conducive to corrosion resistance improvement of Mg alloys, their industrial application is still restricted [13]. In view of the special corrosion properties and dual phase structures of AZ91D alloy, two primary factors decide its corrosion resistance [16-19]. One is the corrosion resistance of a-phase matrix, which is strongly affected by its microstructure and aluminum concentration. The other is the volume fraction and morphology of b-phase, which can act as the cathodes in micro-galvanic cells to accelerate corrosion but the corrosion barriers to retard corrosion propagation in a-phase matrix. Since the ECAP process will severely change the microstructure of a-phase matrix as well as the morphology and distribution of b-phase, the ECAPed AZ91D alloy may present entirely different corrosion behavior compared to the as-cast one.

International Journal of Applied Engineering Research ISSN 0973-4562 Volume 10, Number 23 (2015) pp 43649-43654

2. Experimental Procedure

The base metal used in this investigation is a cast alloy of AZ91D magnesium alloy of 12 mm thickness. The chemical composition of the base metal was obtained using Energy Dispersive Spectrometry (EDS). The chemical composition of the base metal in weight percent is given in Table. 1.

Table1: Base Metal in weight percent

Material	Al	Mn	Zn	Si	Fe	Cu	Ni	Mg
Base Metal (AZ91D)	**9. 1**	**0. 15**	**0. 84**	**0. 10**	**0. 005**	**0. 03**	**0. 002**	**Bal.**

2.1 Procedure for Mechanical Testing

Tensile specimens were prepared as shown in Figure 1 to obtain the base metal tensile properties. ASTM E8M-90a (ASTM, 1991a) guidelines were followed for preparing the test specimens. Tensile tests were carried out in 100 kN, electro-mechanical controlled Universal Testing Machine (Make: FIE-BLUE STAR). The specimen was loaded at the rate of 1. 5 kN/min as per ASTM specifications so that tensile specimen undergoes deformation. The specimen finally fails after necking and the load versus displacement was recorded. The 0. 2% offset yield strength was derived from the diagram. The percentage of elongation also evaluated and the values are presented.

The base metal used in this investigation was 10 mm thick cast plate of AZ91D magnesium alloy. The top surface of cast alloy was friction stir processed to 5 mm deep on a retrofitted milling machine. The FSP experimental setup is carried out straight cylindrical friction stir tool (pin length 5 mm, pin diameter 5 mm, shoulder diameter 15 mm) made of high carbon steel was used in the present study. A tool rotational speed of 1000 rpm and travel speed of 40 mm/min, were employed and processed alloy AZ91D.

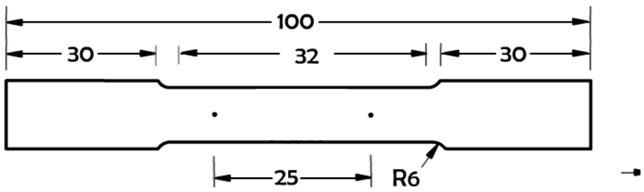

mm

Figure. 1 Tensile specimen

2.2. Procedure for Tensile Test

After FSP, the tensile specimen was prepared (as shown in Figure. 2) along the weld direction (in the processed alone) and loaded at the rate of 1. 5 kN/min as per ASTM specifications, so that tensile specimen undergoes deformation in tensile testing machine. The specimen finally fails after necking and the load versus displacement was recorded. The 0. 2% offset yield strength was derived from the diagram. The percentage of elongation also evaluated. Except the loss of effective loaded area, stress concentration is the governing factor to the drop of corrosion residual strength. As an inductile material, AZ91D magnesium alloy is easily suffering damage from stress concentration especially at the corrosion pits, which leads to the emanation of cracks. As indicated in Fig. 3(a), the max stress (σmax) at the tip of corrosion pit has already achieved the fracture stress of the matrix as a result of the emergence of stress concentration; however, the mean stress of the test bar is far lower than the fracture stress of the matrix at the fracture moment. It is the reason why the failure of magnesium alloy happens at low stress when the test sample suffered corrosion before the loading process. In order to make a better understanding of stress concentration caused by corrosion, stress concentration factor (ksc) is introduced to estimate the stress concentration quantitatively. The stress concentration factor can be mathematically expressed as follows:

$$ksc = \sigma f / \sigma CRS \quad (1)$$

In Eq. (1), σf is the fracture stress; σCRS is the corrosion residual strength; ksc is the stress concentration factor. Stress concentration factor versus EDCP is shown in Fig. 3(b). The result indicates that the unmodified AZ91D magnesium alloy is easily suffered a higher stress concentration than the 1. 0 wt. % Y modified AZ91D magnesium alloy. Additionally, it also reveals that stress concentration factor is closely related to EDCP.

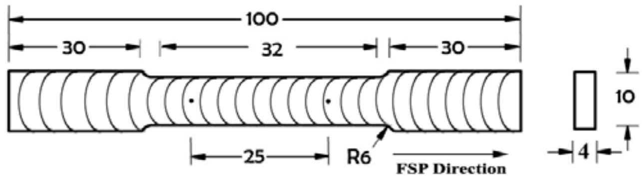

mm

Figure. 2 Tensile specimen prepared after FSP

(a)

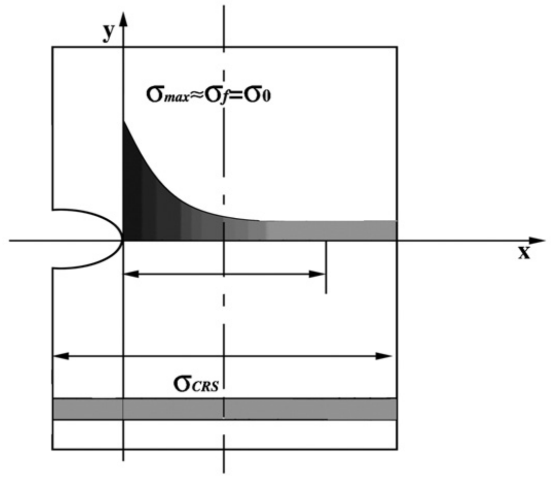

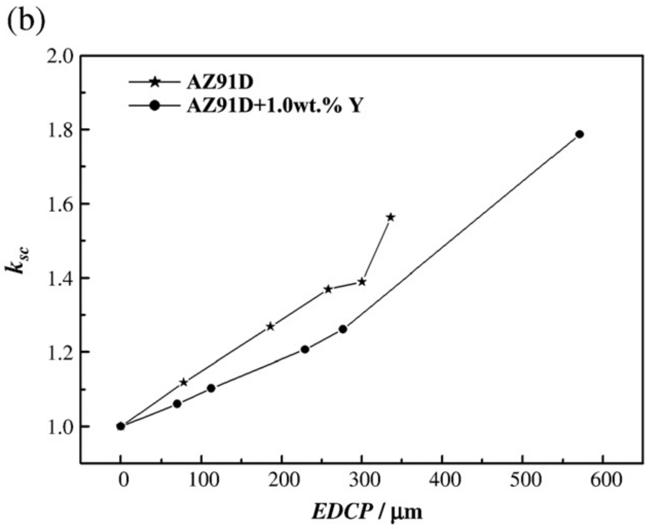

Fig. 3-(a) Diagrammatic sketch of stress concentration emerging at the tip of corrosion pit and (b) the variation of the stress concentration factor (ksc) versus EDCP.

3. Corrosion Rate and Its Behaviour

Corrosion behavior of the ECAPed AZ91D alloy was investigated by three methods, namely in-situ corrosion observation, constant immersion test and electrochemical tests. The cast AZ91D alloy was also studied for comparison. With immersion time increasing, the corrosion residual strength of the unmodified AZ91D magnesium alloy and the 1. 0 wt. % Y modified AZ91D magnesium alloy drops continuously. Surface breakdown caused by corrosion should be responsible for the drop of corrosion residual strength. As is well known, corrosion is commonly classified as uniform corrosion and local corrosion judging from corrosion morphology. In the presence of Cl−, pitting corrosion is the main corrosion mode, which is a typical mode of the local corrosion. And therefore pitting corrosion plays an important role in causing the drop of corrosion residual strength to the AZ91D magnesium alloy. All the experiments were conducted in the 3. 5 wt% chloride sodium solution at room temperature, and the solution was prepared using A. R. grade NaCl in distilled water. In in-situ corrosion observation, one surface of each sample was put a droplet of 3. 5 wt% NaCl and then concomitant corrosion phenomenon under the tiny droplet was monitored via a XJG-05 digital microscope. For constant immersion tests, the specimens were abraded with emery papers up to 1000 level and cleaned according to the procedure of ASTM standard G-I-72. The polished and weighed samples were immersed in the 3. 5 wt% NaCl solution, cleaned with a20 wt% CrO3 + 1 wt% AgNO3 solution at 353 K, washed with acetone again. The above steps were repeated and the mass loss in every interval was measured to evaluate the corrosion rate of ECAPed samples (Unit: mg cm_2 h_1). After every corrosion period, surface macro-and micro-morphologies were observed by a KH-7700 digital microscope (Hirox, USA) and a scanning electron microscopy (Hitachi S340-N, Japan), respectively are shown in figure. 3(a& b).

Electrochemical tests were conducted in 3. 5 wt% NaCl solution via a Parstat 2273 advanced potentiostat with a traditional three electrode system. The system contains a saturated calomel reference electrode and a Pt counter electrode. Herein, all samples were cut from the core of ECAPed billets perpendicular to the pressing direction by electric discharging machine, and then molded in the epoxy with an exposed surface of 1 cm2. For a good reproducibility, all samples were polished, cleaned with acetone and dried in warm air, and at least three replicates were run for each sample. Three kinds of electrochemical tests, namely open circuit potential test (OCP), potentio dynamic polarization test and Electrochemical Impendence Spectroscopy test (EIS), were carried out to compare corrosion resistance of ECAPed samples with that of the as-cast sample. Considering the original poor corrosion resistance of AZ91D alloy, the set immersion time of OCP tests was 300 s, the Potentio dynamic polarization tests were carried out at a relatively high scan rate of 5 mV s_1. The frequency of EIS tests ranged from 10 kHz to 10 mHz, whereas the amplitude of the sinusoidal potential signal was 5 mV with respect to the open circuit potential.

4. Results and Discussion

4. 1 Micro structure

The optical and scanning electron micrographs of friction stir processed AZ91D cast magnesium alloy are presented in Figure 4(a) & (b). The microstructure of BM is mainly composed of α-Mg dendrites and coarse eutectic β-$Mg_{17}A_{12}$ phase. Most of the β-$Mg_{17}A_{12}$ phase exist as network structure, while some particles are distributed inside a grains. The average grain size of α-Mg is determined to be about 140 μm. The nugget zone of the FSP AZ91D is characterized by fine grains (4 μm) and fine particles distributed at the grain boundaries in Figure 5(a) &(b). In contrast to previous studies, fine particles were found within the grain interior by SEM examinations under a high magnification. The coarse eutectic β-$Mg_{17}A_{12}$ network in the as-received AZ91D disappeared after FSP. Friction stir processing resulted in significant breakup and dissolution of the network like eutectic β-$Mg_{17}A_{12}$ phase due to the stirring effect of the threaded pin and thermal exposure. The observed structures suggest the mechanisms that lead to the strong reduction in the size and fraction of β phase in the nugget are more complex than mechanical attrition/solid state dissolution as commonly supposed.

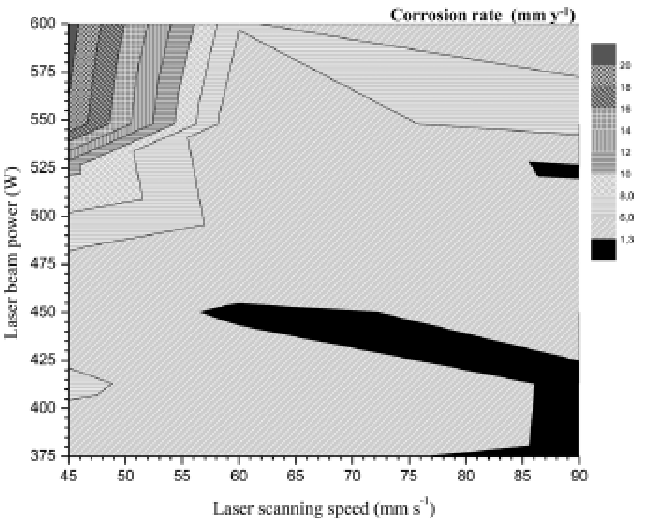

(a)

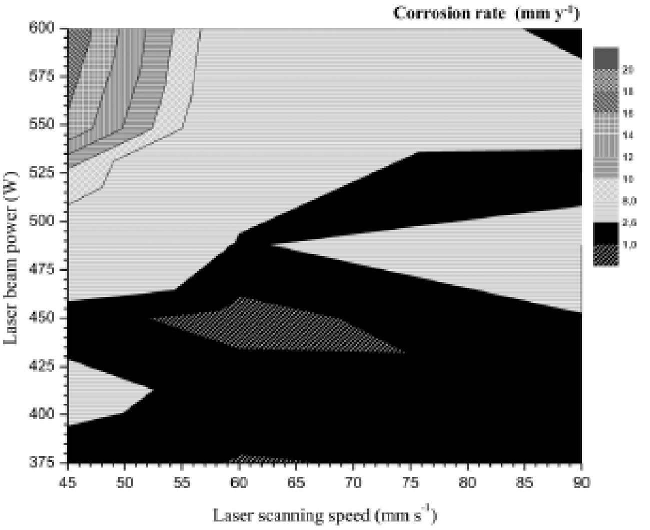

(b)

Figure 4 a) corrosion rate evaluated at the longer immersion times, b) some of the samples had corrosion rates lower than the average of the corrosion rate for AZ91D.

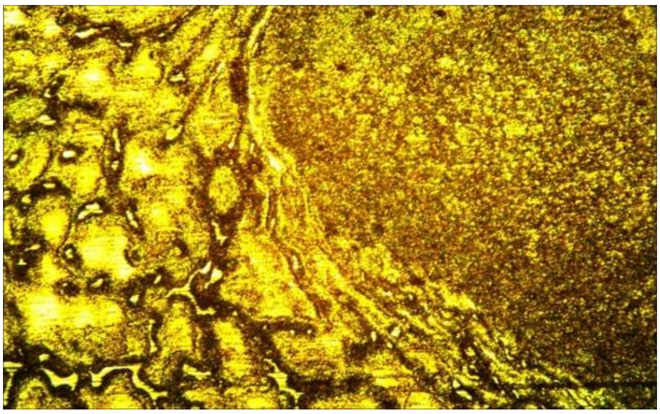

(a)

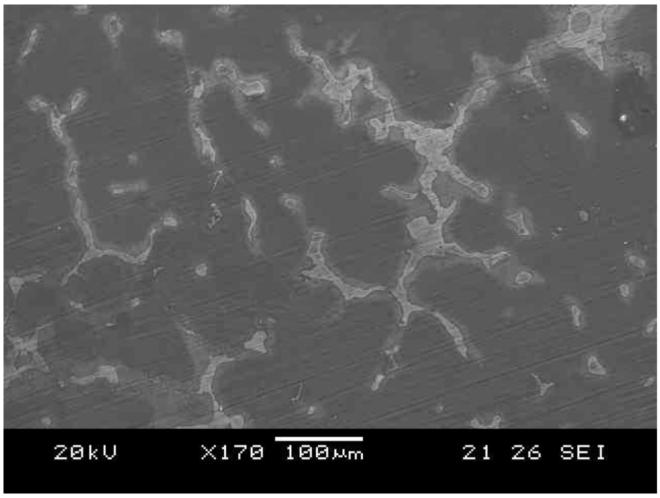

(b)

Figure 5 a) Optical micrograph of AZ91D after FSP b) Scanning electron micrograph of base metal

4. 2 tensile properties and corrosion observation

The tensile properties such yield strength, tensile strength and percentage elongation were measured from the samples prepared from friction stir processed region of AZ91D alloy. A microstructure of ECAPed AZ91D alloys. the corrosion features of the AZ91D alloy samples with different ECAP passes after in-situ corrosion for 10 min: (a) as-cast state; (b) 1 pass; (c) 4 passes; (d) 8 passes and (e) 12 passes. The in-situ corrosion experiments were carried out to observe the initial corrosion behavior and the breakdown of the partial protective film on the AZ91D alloy surface. the partial protective film (composed with Mg(OH)2 mainly) immediately forms on the surface of Mg sample when it contacts an etching solution. And at the same tine, hydrogen evolution starts. It means that the film formation and its breaking are to take place simultaneously at the initial corrosion stage. The initial corrosion behavior of AZ91D alloy is the irregular pitting corrosion in the means of film break on the a-phase matrix in the vicinity of the b-phase. Compared to the cast AZ91D alloy, the ECAPed samples has more pit numbers but smaller pit sizes, and those numbers of pits were connected and distributed along the plastic flow. This phenomenon became more marked with the increase of ECAP passes, and more corroded areas could be found in the samples with more ECAP passes. The results are compared with the various structure base metals. It is observed that after friction stir processed AZ91D magnesium alloy superior tensile properties compared to the base metal and it is mainly due to the fine grain structure with uniform distribution of β phase. The macro-morphologies of ECAPed and as-cast AZ91D alloys it is clear that the corrosion resistance of the ECAPed AZ91D alloy is weaker than that of the as-cast sample, and the more ECAP passes the weaker corrosion resistance is. In comparison with the cast AZ91D sample, there are two special corrosion features which can be found from the ECAPed AZ91D samples. Comparison has been made with various tensile FSped for the base metal AZ91D magnesium alloy as shown in figure. 7

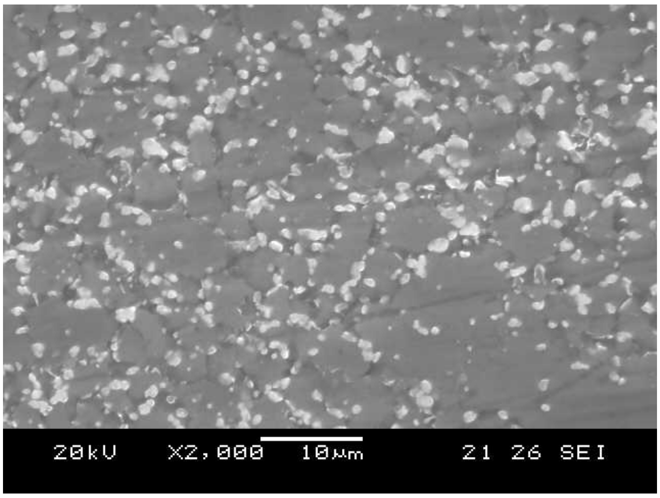

Figure 6 Scanning electron micrograph of base metal

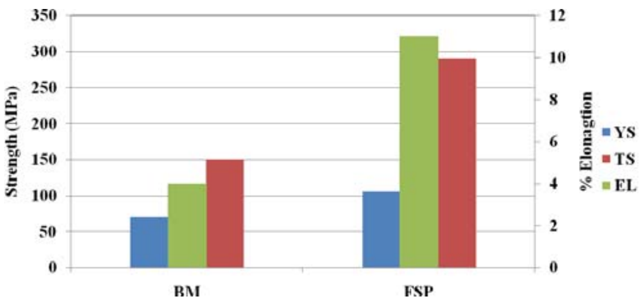

Figure. 7 Tensile properties of FSPed AZ91D magnesium alloy

5. Conclusion

This investigating carried the influence of processing parameters on the corrosion and tensile of behaviour magnesium alloy AZ91D using efficient electron microscope.

- The grained AZ91D magnesium alloy was achieved through equal channel angular pressing and subsequently tested. There was homogeneous corrosion attack and the formation of a thin surface layer for middle input energy LSM treatments, implying a modification of the corrosion morphology of the as-received AZ91D.
- The corrosion rate decreased up to 97% by using magnesium alloy AZ91D. These results reveal from analysis had more influence on the corrosion of the treated samples than the micro-structural modifications achieved.
- After grinding, the corrosion rate of the samples was up to 70% lower than those of the untreated AZ91D. This indicates that the modification of the microstructure has a positive effect in the corrosion evolution of AZ91D is a useful method to improve the corrosion resistance of the AZ91D alloy.
- The results analysis of tensile properties such as yield strength, ultimate tensile strength, percentage of elongation and micro-hardness properties obviously imply AZ91D magnesium alloy and their tensile behavior suggests that is better than conventional magnesium alloys.

In proposed system the delay to reach the energy information of sensor is lesser when compared to the hierarchical order of the nodes in the wireless sensor network, because in cluster there is no more no of intermediate nodes to receive and send the neighbor nodes energy message.

References

[1] Christopher A., Walton, Holly, J. Martin, M. F. Horstemeyer, Wilburn R., Whittington, C. J. Horstemeyer, Paul T. Wang, "Corrosion stress relaxation and tensile strength effects in an extruded AZ31 magnesium alloy", Corrosion Science, Volume 80(2014), Pages 503-510.

[2] Tada, N. and Masago, H. , "Evaluation of tensile strength of copper-cored lead-free solder joints in air, distilled water, and NaCl solution using testing device with permanent magnets", International conference in Microsystems, Packaging, Assembly and Circuits Technology Conference (IMPACT), Taiwan, 2014.

[3] Srinivasa Rao, K. , "Friction stir processing for enhancement of stir resistance of ZM21 magnesium alloy", Transactions of the Indian Institute of Metals 66 (2013), pp. 13-24.

[4] Chai, F. , Zhang, D. , Zhang, W. , Qiu, C. , "Effect of processing speed on microstructures and mechanical properties of submerged friction stir processed AZ91 alloy" Materials Science Forum, (2011) pp. 276-281,

[5] Jain, V. , Mishra, R. S. , Gupta, A. K. , Gouthama, "Study of B-precipitates and their effect on the directional yield asymmetry of friction stir processed and aged AZ91C alloy", Materials Science and Engineering A Vol. 560(2013), pp. 500-509.

[6] Govindaraju, M. , Prasad Rao, K. , Chakkingal, U. , Balasubramanian, K. , "Effect of distance between passes in friction stir processing of magnesium alloy", Advanced Materials Research Vol. 585(2012), pp. 397-401.

[7] Arora, H. S. , Singh, H. , Dhindaw, B. K. , Grewal, H. S. "Improving the tribological properties of mg based AZ31 alloy using friction stir processing", Advanced Materials ResearchVol. 670 (2013), pp. 579-583.

[8] Mansoor, B. , Ghosh, A. K. , "Microstructure and tensile behavior of a friction stir processed magnesium alloy", Acta Materialia, Vol. 60 (2012), pp. 5079-5088.

[9] Du, X. , Zhang, E. , Wu, B. , " Achieving ultra-fine grains in AZ61 Mg alloy by friction stir processing" International Journal of Materials Research, Vol. 99 (2008), pp. 1375-1378.

[10] Lu, Q.-Y. , Sha, G.-Y. , Wang, H. Hangkong, Cailiao Xuebao, "Microstructure and properties of friction stir-processed AZ91 magnesium alloy", Journal of Aeronautical Materials, Vol. 28 (2008), pp. 27-30.
[11] T. Morishige, M. Tsujikawa, M. Hino, T. Hirata, S. Oki and K. Higashi, "Microstructural modification of cast Mg alloys by friction stir processing, International Journal of Cast Metals Research" Vol. 21 (2008) pp. 1-4.
[12] Sung Jin Kim, Hwan Gyo Jung and Kyoo Young Kim, "Effect of tensile stress in elastic and plastic range on hydrogen permeation of high-strength steel in sour environment", Electrochemical Acta, Volume 78(2012), Pages 139-146.
[13] Liu Jin, Xiuli Du, Guowei Ma, "Macroscopic effective moduli and tensile strength of saturated concrete, Cement and Concrete Research", Volume 42, Issue 12(2012), Pages 1590-1600.
[14] Peng G, Chen K, Chen S, Fang H. "Influence of repetitious-RRA treatment on the strength and SCC resistance of Al-Zn-Mg-Cu alloy". Mater Science Eng-AVol. 97 (2011), pp. 1245-1251.
[15] Su, C. L., Xin, L. and Jing, Z. "Numerical Analysis of Ultimate Benging Capacity of Pipeline with Single Corrosion Defect". The 20th national structure engineering academic meeting. 360-367, 2011.